Feasibility Study on the Design of a Laminar Flow Nacelle

R. Radespiel,* K. H. Horstmann,† and G. Redeker‡
Deutsche Forschungsanstalt fuer Luft-Und Raumfahrt (DLR), Braunschweig, Germany

This paper describes the design of a laminar flow nacelle using numerical flow methods. With an appropriate contouring of the nacelle, natural laminar flow is maintained up to 60% of the nacelle length at cruise flight conditions. The drag reduction that is obtained if a transport aircraft is equipped with two laminar flow nacelles instead of conventional turbulent nacelles is estimated at $\Delta C_{D,A/C} = 0.0011$. The behavior of the laminar flow nacelle is also investigated for takeoff and landing conditions. It is found that the inlet of the new nacelle is not more sensitive to flow separation than conventional nacelles.

Nomenclature

A = area
A_{HL} = highlight area, = 5.8 m^2
$C_{D,A/C}$ = drag coefficient of aircraft based on wing area
C_{DV} = viscous drag coefficient of nacelle, $= D_V/(\rho/2v^2_\infty A_{HL})$
C_{dV} = viscous drag coefficient of section
C_{DW} = wave drag coefficient of nacelle, $= D_W/(\rho/2v^2_\infty A_{HL})$
c = chord length of nacelle, = 3.152 m
c_p = pressure coefficient, $= (p-p_\infty) / (\rho/2v^2_\infty)$
M = Mach number
$\dot{m}$ = mass flow
p = pressure
T = temperature
v = flow velocity
x,y,z = components of Cartesian coordinates
γ = ratio of specific heats, = 1.4
δ_2 = momentum thickness
ϵ = area ratio A_∞/A_{HL} of the streamtube of the flow through the nacelle
θ = angle in circumferential direction
ρ = density

Subscripts and Superscripts

A/C = aircraft
∞ = infinity
0 = stagnation value
( )* = critical value
j = jet
t = trailing edge

Introduction

IT is well known that the economy of transport aircraft is related strongly to its aerodynamic drag. The introduction of laminar flow over large parts of the aircraft surface is a promising way to reduce the drag. Earlier studies[1] have shown that a drag reduction of almost 30% is possible if the wing and the empennage are designed to allow natural laminar flow.

Future generations of transport aircraft will use engines with bypass ratios on the order of 20. Then the surface of the engine nacelles is considerably large in comparison to the wing area. Thus, applying the laminar flow technology to engine nacelles is a promising means to reduce aircraft drag.

The present work deals with the design of a laminar flow nacelle for given design conditions and given overall geometry data. The first part of this paper describes the methods used herein; the second part deals with the design process. Finally, the performance of the new nacelle is investigated at different flow conditions corresponding to cruise, takeoff, and landing. The consequences with respect to overall aircraft drag reduction are estimated, and new technical problems, which arise when laminar flow nacelles are integrated into a transport aircraft, are covered briefly.

Analysis and Design Methods

In the present study, the principal feasibility of designing a laminar flow nacelle for typical flow conditions of modern transport aircraft is considered. For this purpose, the investigations are restricted to isolated and axisymmetric nacelles. Note that the final design of a nacelle to be installed close to the wing should take into account wing-pylon interference effects.

When calculating the transonic flow around an isolated nacelle, one can make use of the fact that the boundary layers along the nacelle contour are thin except in the region of the trailing edge. Furthermore, the flow around the nacelle is not very sensitive to the Kutta condition at the trailing edge, as in the case of the plane airfoil flows. The flow around the inlet of a nacelle mainly depends on the mass flow into the inlet, which is generally prescribed by the engine manufacturer and is not influenced significantly by viscous effects. These considerations justify the use of a first-order boundary-layer theory, where the pressure distribution along the nacelle is governed by the inviscid flow around the nacelle. The boundary layers are determined by the pressure distribution of the inviscid flow, and their interaction with the inviscid flow is negligible.

Analysis Method for Transonic Inviscid Flows Around Isolated Nacelles

For the analysis of the transonic inviscid flow around isolated nacelles, an extension of the three-dimensional DLR Euler code called CEVCATS[2] is used. This code is based on a cell-vertex finite-volume scheme for the three-dimensional Euler equations. The scheme uses central differences for the calculation of the flux balances, and, therefore, artificial dissipative terms are used to damp high-frequency oscillations in the solution. Steady-state solutions are obtained by using a Runge-Kutta time-stepping scheme. The convergence criterion used here is the reduction of the root-mean-square (rms) of the residual by four orders of magnitude. The scheme is analyzed in detail in Ref. 3. The extension of CEVCATS for the calculation of nacelle flows is described in Ref. 4.

Presented as Paper 89-0640 at the 27th Aerospace Sciences Meeting, Reno, NV, Jan. 9–12, 1989; received April 19, 1989; revision received April 9, 1990.

*Head, Aerothermodynamics Section, Institute for Design Aerodynamics.
†Research Scientist, Institute for Design Aerodynamics.
‡Head, Airframe Aerodynamics Section, Institute for Design Aerodynamics.

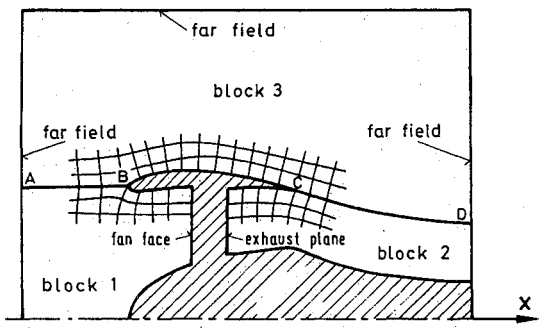

Fig. 1 Sectionwise grid structure for high-bypass nacelle configuration.

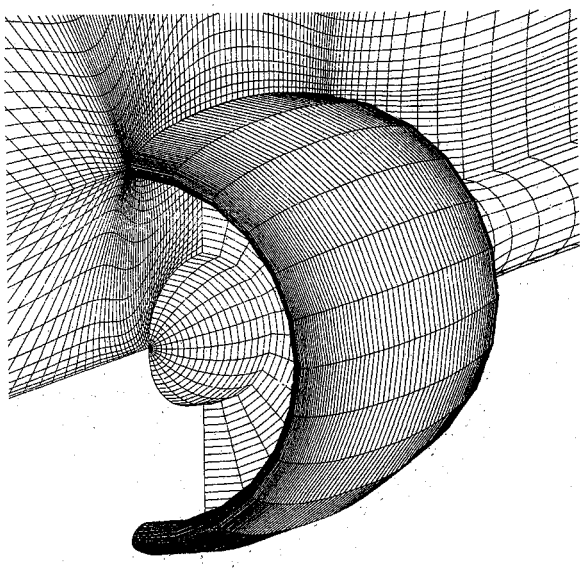

Fig. 2 Enlarged view of nacelle grid in symmetry plane.

The computational domain around the nacelle is divided into three blocks, as sketched in Fig. 1. In the streamwise direction, an H-type grid topology is used, whereas a polar grid is used in the circumferential direction. In the present version of the code, the grid is rotationally symmetric and the core jet is simulated by a cylindrical body. A view of a typical grid section is shown in Fig. 2. The total number of grid points is around 56,000. Note that the three-dimensional Euler code CEVCATS is not restricted to axisymmetric geometries. For an axisymmetric nacelle at transonic flow with 0-deg angle of attack, it produces an axisymmetric flow within the tolerance $\Delta c_p = 0.01$. It was shown in Ref. 4 that the code accurately reproduces the mass flow into the inlet of the nacelle as specified by input.

The accuracy of Euler codes can be judged by using the total pressure loss of the computed flow. For this purpose, the distributions of pressure coefficient and total pressure loss along the nacelle LN1C (see next subsection) are given in Fig. 3 for two different grid densities. In the flow region upstream of the shock, the error in total pressure is much smaller with the fine mesh than with the coarse mesh. The results of the fine grid show that the total pressure loss at the wall is below 1%, except for a small peak at the leading edge with a maximum loss of 2%. Furthermore, it is found by numerical experimentation that the flow solution is not sensitive to the value of the artificial-dissipation coefficients. Moreover, the same coefficients are used for all flow computations. In Ref. 4, the influence of the jet parameters on the flowfield around the nacelle is also investigated.

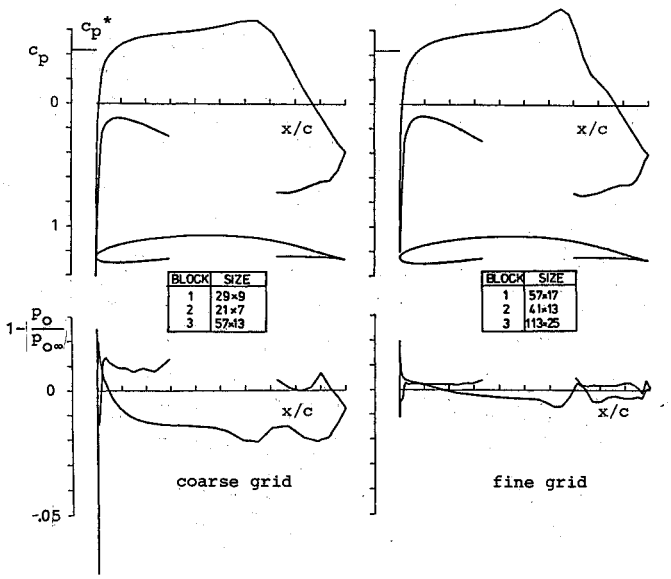

Fig. 3 Distribution of pressure and total pressure loss on a nacelle in axisymmetric flow ($M_\infty = 0.8$, $p_{0j}/p_\infty = 1.52$, $T_{0j}/T_\infty = 1.0$, and $\epsilon = 0.76$).

Analysis Method for Laminar and Turbulent Boundary Layers

For the calculation of laminar and turbulent compressible boundary layers, an integral method according to Rotta[5] is used. The method is based on the numerical integration of the integral equations for momentum and energy. The code can be used for axisymmetric or plane flows. In the axisymmetric case, both external and internal flows can be calculated.

The use of an axisymmetric boundary-layer code is certainly justified under cruise conditions, where the angle of attack is less than 1.5 deg. For the takeoff case, however, a much larger angle of attack is specified and three-dimensional boundary layers within the inlet are expected. In this case, the result of an axisymmetric boundary-layer code is of less value. The behavior of the flow in the takeoff case is discussed further subsequently.

Transition-Location Prediction Method

The location of the transition of the laminar boundary layer into a turbulent boundary layer is predicted by using the stability theory of laminar boundary layers. This method computes the amplification rates of boundary-layer waves, starting at the location of neutral stability. If the logarithm of the amplification rate, called the N factor, exceeds a limiting value that has been determined empirically, transition is predicted, as shown in Fig. 4. The calculation must be done for different combinations of wavelengths and frequencies to find the most amplified wave. The boundary-layer stability code used here, SALLY, is published in Ref. 6. The overall transition prediction technique is described in detail in Ref. 7.

For an application of this two-dimensional transition-location prediction procedure, it is necessary to investigate the influence of three-dimensional effects due to an axisymmetric geometry on the laminar boundary layer. This has been done in Ref. 8 with the Rotta method.[5] The main result of Ref. 8 is that, for a relative nacelle radius of $y/c \geq 0.5$, the differences of the integral boundary-layer parameters between the axisymmetric flow and the two-dimensional flow are negligible.

Drag Prediction Method

Using the present Euler code for the inviscid flow around

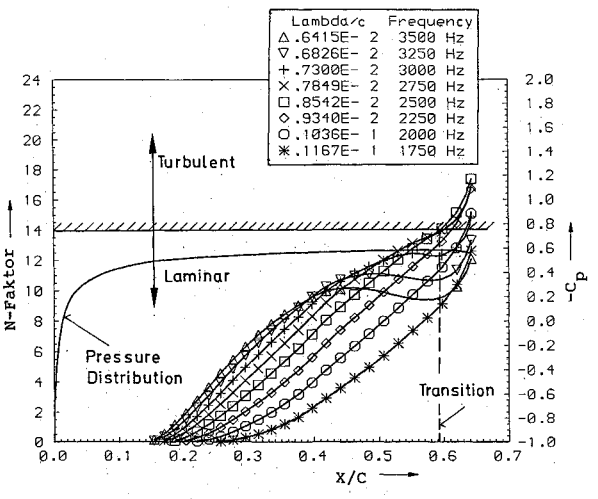

Fig. 4 Prediction of transition location by using stability analysis ($M_\infty = 0.76$, $\alpha = 0$ deg, $\epsilon = 0.76$, and $Re = 20 \times 10^6$).

the nacelle, a direct integration of the pressure drag is not possible for two reasons:

1) The contour of the nacelle is not closed, as shown in Fig. 1. The flow area at the fan face is not the same as at the exhaust plane, because the mass flow of the core jet is included in the inlet and a solid body is used to simulate the core jet.

2) The present Euler code does not account for the pressure drag due to viscous-inviscid interaction. For typical transonic airfoils at design flow conditions, it is known that the pressure drag due to viscous-inviscid interaction is on the order of 40% of the total drag. Therefore, we expect that this pressure drag cannot be neglected when designing a laminar-flow nacelle.

Conversely, it is possible to calculate the total viscous drag from the boundary-layer results at the trailing edge, according to Squire and Young,[9]

$$C_{dv} = (2\delta_2/c)\ (v_t/v_\infty)^{3.2} \tag{1}$$

where c is the chord length of the nacelle and v is the absolute value of the flow velocity. Squire and Young[9] use empirical findings to obtain the momentum loss at infinity from the value at the trailing edge, as given in Eq. (1). Moreover, Eq. (1) was derived for plane two-dimensional flows. We anticipate that it should give reasonable estimates of the viscous drag for the present class of flows around axisymmetric nacelles where the ratio of the momentum thickness δ_2 over the nacelle radius at the trailing edge is typically 0.005–0.01. Equation (1) is applied to calculate viscous pressure drag and friction drag of the outer flow around the nacelle, starting from the stagnation point at the leading edge and ending at the trailing edge. Hence, it is possible to estimate the drag increment between nacelles with laminar and turbulent flow. Note that the ratio of the flow velocity at the trailing edge v_t/v_∞ contributes significantly to the drag in Eq. (1). If inviscid flow methods are used to determine the pressure distribution, and with it v_t at the trailing edge, the viscous drag C_{dV} generally is underpredicted.

Furthermore, the wave drag due to shock waves in transonic flow is neglected in Eq. (1). Experiences with transonic airfoils indicate that the wave drag is negligible in comparison with the viscous drag if the Mach number upstream of the shock does not exceed $M = 1.15$. At higher Mach numbers, where the local Mach number upstream of the shock wave is larger, the wave drag is roughly estimated by subtracting the pressure drag at a lower Mach number without shock from that at the high Mach number.

Table 1 Design points of a laminar flow nacelle

Design Point	M_∞	α, deg	$\epsilon = A_\infty/A_{HL}$	Re, $\times 10^6$
Cruise	0.80	0–1.5	0.76	20
Takeoff	0.25	18	1.4	20
Landing	0.30	9	0.2	20

The drag values given next have been made nondimensional with the highlight area A_{HL}:

$$C_D = C_{dV}\, 2\pi\, y_t\, c/A_{HL} \tag{2}$$

where $A_{HL} = 5.8$ m^2 and the trailing-edge radius y_t was fixed throughout the present work at $y_t = 1.32$ m.

Design Method for Fan Cowl Contours

In the present study, fan cowl contours have been designed with a low-speed design method for airfoils according to Eppler and Somers.[10] The design procedure determines a conformal mapping so that constant pressure is obtained over specific regions of the airfoil at specified angles of attack. Of course, this is true for incompressible plane flow only, and the pressure distribution for three-dimensional transonic flow around a nacelle may be quite different from that of the low-speed airfoil.

Nevertheless, the angle of attack in the design code can be chosen so that the stagnation points on the low-speed airfoil and on the transonic nacelle coincide. Then, the flows around the nose of the airfoil and the nacelle behave very similarly and the input parameters of the airfoil design code can be used systematically to change the transonic behavior of the nacelle. With some experience, the flow around the nacelle can be influenced effectively by changing the input of the low-speed code.

Nacelle Design with Natural Laminar Flow on Fan Cowl

Design Conditions

For the design of a natural laminar flow nacelle, three design points have been taken into account. These are shown in Table 1. The design points are characterized by the Mach number, the Reynolds number, a range of angle of attack, and the mass flow ratio ϵ, which is defined by the ratio between the area of the inlet streamtube at infinity and the highlight area of the nacelle.

Design Process

The design of the nacelle contour has been done iteratively by using the design and analysis methods described earlier. The different steps in the design process are listed here.

1) Choice of a subsonic velocity distribution which is assumed to fulfill the design requirements, taking into account the two-dimensional subsonic and three-dimensional transonic calculations of a nacelle contour given by an iteration step before, or, in case of initialization of the design process, by a conventional nacelle.

2) Calculation of a nacelle contour using the two-dimensional subsonic design code.[10]

3) Reiteration of steps 1 and 2 until the desired pressure distribution characteristics in the different design points are obtained.

4) Calculation of the three-dimensional transonic inviscid pressure distribution at the design points by the Euler code.[4]

5) Reiteration of steps 1–4 until a desired transonic pressure distribution is obtained.

6) Calculation and prediction of the laminar/turbulent transition using the stability code[6,7] and calculation of the boundary-layer characteristics using the Rotta method.[5]

7) Reiteration of steps 1–6 until the design objectives at different design points are fulfilled.

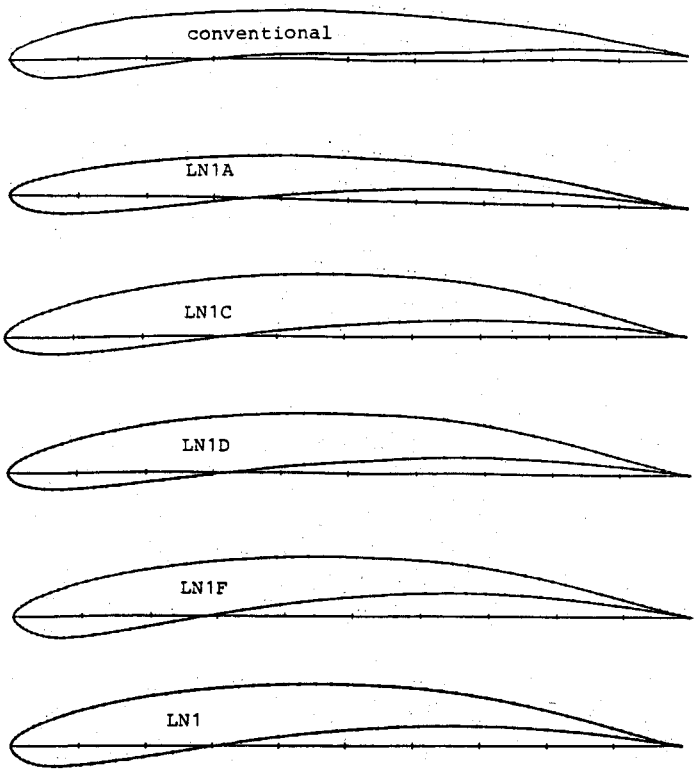

Fig. 5 Nacelle contours at various stages of the design process.

This manually controlled design process is effective in computing time because the changes from step to step in all of the design points are very purposive. However, we concede that certain airfoil design experiences are necessary to handle this process.

Some nacelle contours and related pressure distributions that occurred in various steps of the design process are discussed next. The contours LN1A and LN1D in Fig. 5 show the modifications from the complete adverse outside pressure distribution of a conventional nacelle to a typical natural laminar flow pressure distribution with a slight pressure drop up to 60% of chord length, Fig. 6. The maximum thickness is increased from 7.4 to 9.6%, and the location of maximum thickness is shifted downstream.

Another important design point is the takeoff case with low freestream Mach number and high angle of attack. Figure 7 shows that the inside pressure peak at the $\theta = 180$ deg section can be reduced by a careful design. From LN1D to LN1, the contour curvature is decreased in the supersonic region and increased behind it, resulting in a reduced supersonic expansion.

The computational expense of the design work described here is reasonably low. The subsonic design method and the integral boundary-layer method require almost no computing time. Each three-dimensional computation with the Euler code requires just under 20 min of CPU time on a CRAY XMP-216. Each computation of axisymmetric flow with a simplified version of the three-dimensional Euler code, where only a single plane of the polar mesh is computed,[4] takes about 2–3 min of CPU time. The prediction of transition with the SALLY code takes 6 min of CPU time. In total, 4 h of computation time on a CRAY XMP-216 were spent for the present work.

Analysis of the Aerodynamic Behavior of the Final Design

The finally obtained nacelle contour is named LN1. The aerodynamic characteristics of nacelle LN1 are described subsequently.

Cruise Conditions

The pressure distribution at cruise conditions is the main design objective for a laminar flow nacelle. Cruise conditions are defined by the following values: $M_\infty = 0.8$, $\alpha = 0$ deg, and $\epsilon = 0.76$. In general, it is necessary to have a certain range of flow conditions around the design point where the nacelle works properly. Therefore, pressure distributions at different Mach numbers from 0.70 to 0.84 are shown in Fig. 8. All pressure distributions exhibit a favorable gradient up to 60% of chord length or more. If the freestream Mach number is increased above 0.80, the local Mach numbers upstream of the shock rise drastically.

Transition was predicted downstream of the 60% line for $M_\infty > 0.76$. At $M_\infty = 0.80$, the design objective with respect to transition is fulfilled easily, and there is almost no shock in the flow along the nacelle. Conversely, if cruise Mach numbers above 0.8 are intended, a modified design would be appropriate. For this purpose, the favorable pressure gradient at $M = 0.8$ could be somewhat reduced in order to shift the occurrence of strong shocks to higher Mach numbers. Doing this, the nacelle diameter will be reduced slightly.

A properly designed laminar flow nacelle should also work in a certain angle-of-attack range. Figure 9 shows the influence of the angle of attack ($\alpha = 0$, 1.5, and 4 deg) on the pressure distributions at two characteristic sections of the fan cowling. In most cases, the laminar/turbulent transition on

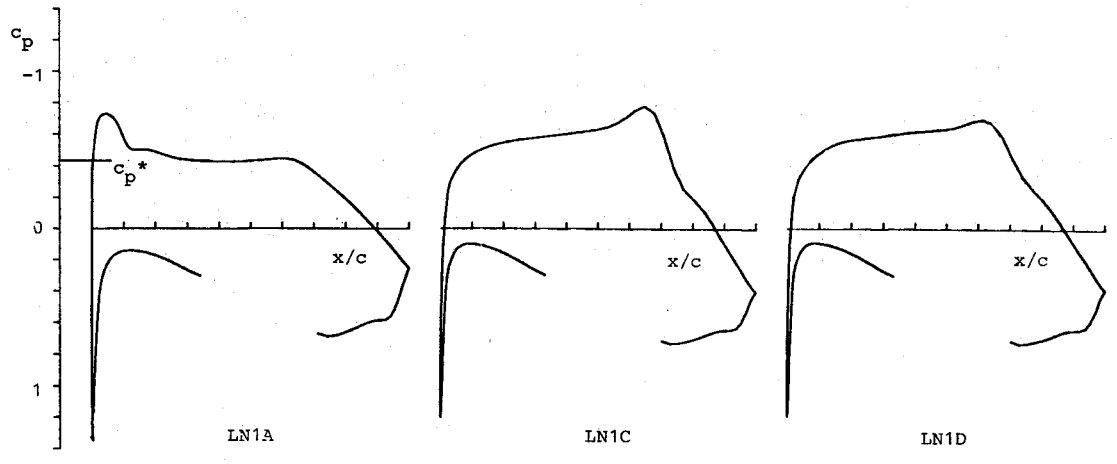

Fig. 6 Pressure distribution for axisymmetric flow around nacelles in cruise ($M_\infty = 0.8$ and $\epsilon = 0.76$).

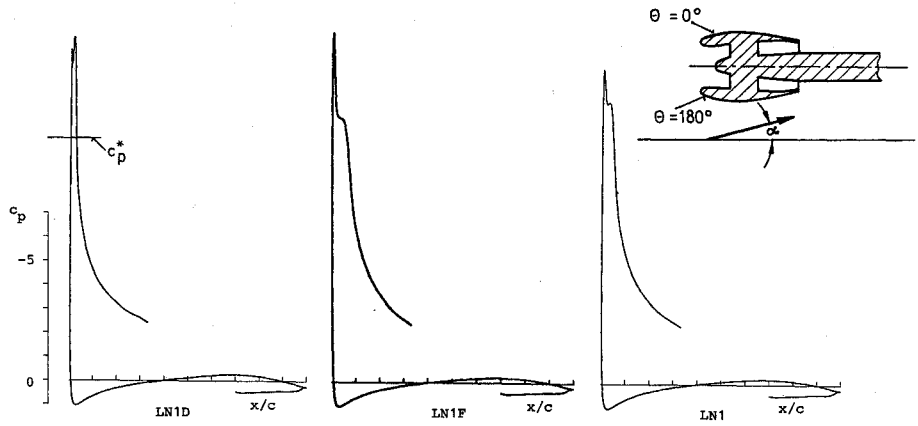

Fig. 7 Pressure distribution on nacelle sections θ = 180 deg at M_∞ = 0.25, α = 18 deg, and ϵ = 1.4.

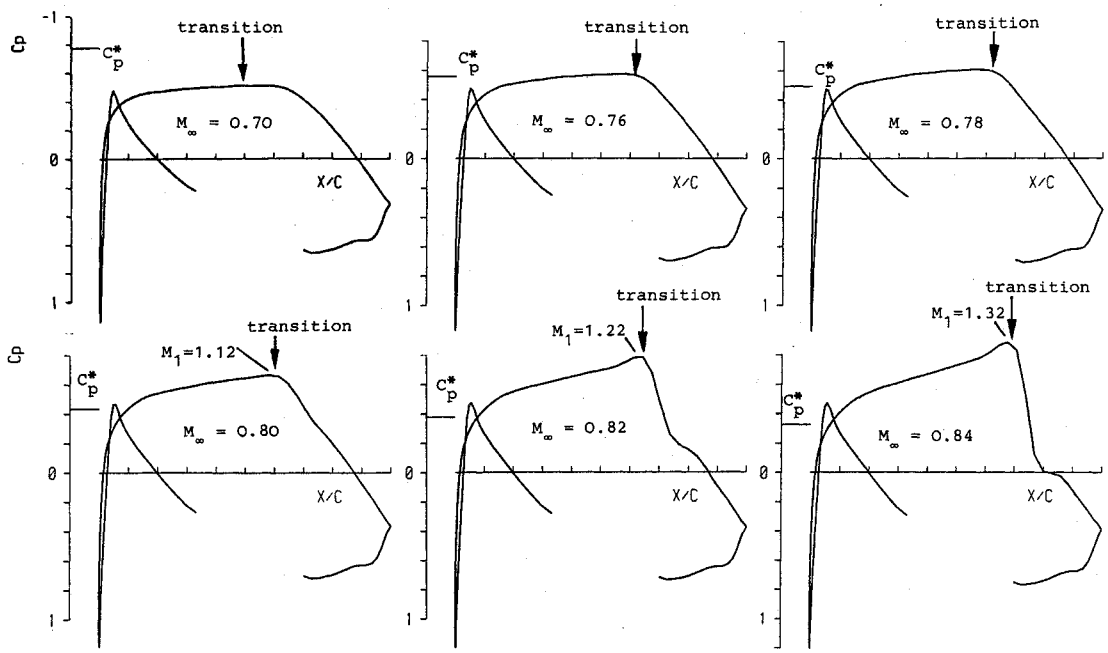

Fig. 8 Influence of Mach number on pressure distribution on nacelle LN1 in cruise (α = 0 deg and ϵ = 0.76).

the outer contour occurs between 60 and 70% of chord length. Only at the θ = 0-deg section, the extension of the laminar boundary layer is reduced to 50% at α = 1.5 deg and to 30% at α = 4 deg. For α = 4 deg and θ = 180 deg, a shock with a maximum local Mach number of M = 1.2 is predicted in the nacelle inlet. The boundary-layer code, however, does not indicate any separation for this flow case.

Takeoff and Landing Conditions

The pressure distributions along three characteristic nacelle sections, i.e., along the upper and lower sides, and in a horizontal plane (θ = 0, 180, and 90 deg) at an angle of attack α = 18 deg and at a maximum thrust (ϵ = 1.4) are shown in Fig. 10. A critical pressure peak appears at the lower inner contour near the leading edge. The maximum Mach number there is M = 1.15. The pressure rise is rather steep, but the pressure level at the fan entrance plane is low, and so the boundary-layer calculation (not shown) does not indicate separation. Recall that the boundary layer is calculated by an axisymmetric code and so the influence of the crossflow cannot be considered. Conversely, computations of the flow along the conventional nacelle contour of Fig. 5 (not shown here) yielded a slightly higher maximum Mach number at that location. Therefore, we conclude that the inlet of the new nacelle is not more sensitive to flow separation than conventional designs. The adverse pressure gradients along the outer contour of the nacelle are relatively small. The transition from laminar to turbulent has not been calculated in the takeoff case because the drag portion of the nacelle is low at takeoff. However, it can be estimated that the fan cowling outside is laminar up to 65% of chord length for 45 deg < θ < 315 deg.

The pressure distributions at landing conditions (M = 0.3, α = 9 deg, ϵ = 0.2) are presented in Fig. 11. A sharp pressure peak is seen near the leading edge at θ = 0 deg, but the boundary-layer calculation does not indicate any separation. The axisymmetric boundary-layer calculation is certainly too optimistic, because the thickness of the boundary layer at θ = 0 deg should be increased significantly by the crossflow of the

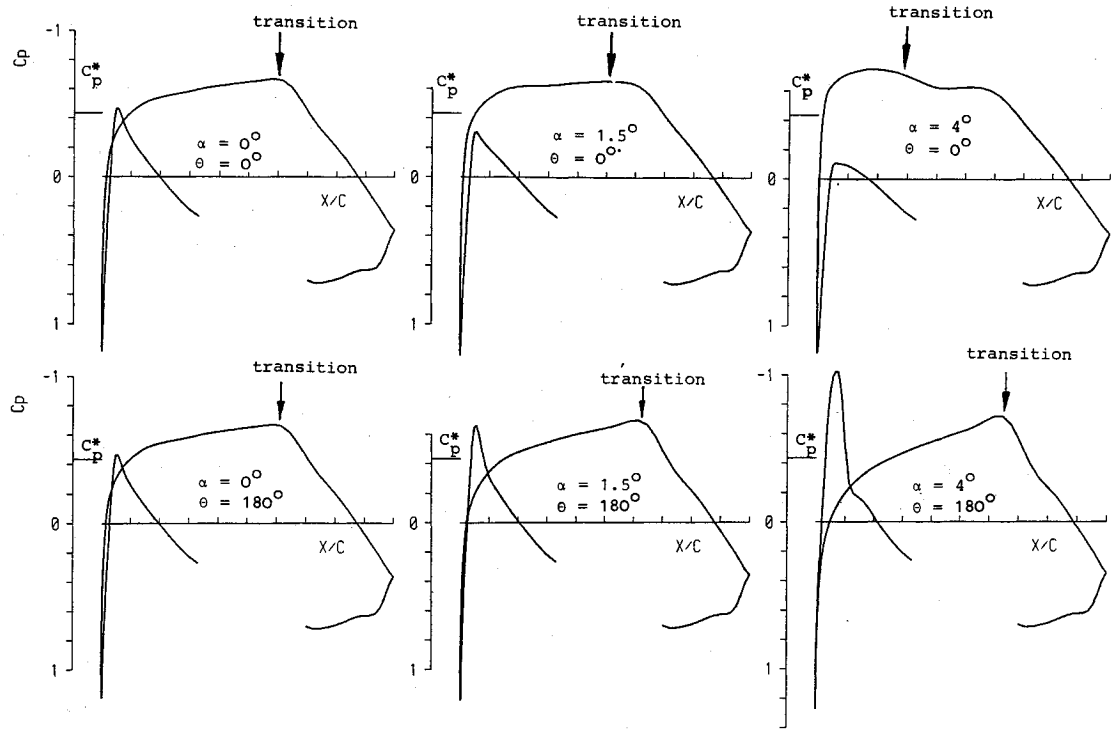

Fig. 9 Influence of angle of attack on pressure distribution of nacelle LN1 ($M_\infty = 0.8$, $\epsilon = 0.76$; $\theta = 0$ and 180 deg).

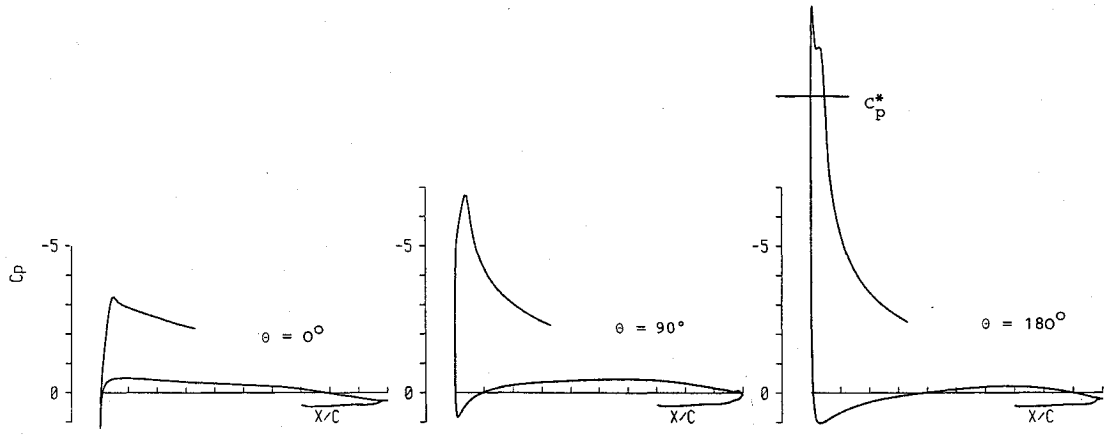

Fig. 10 Pressure distributions on three sections of nacelle LN1 ($M_\infty = 0.25$, $\alpha = 18$ deg, and $\epsilon = 1.4$).

three-dimensional boundary layers. Therefore, some amount of flow separation should be expected for the landing case.

Estimation of Drag Reduction by Laminar Nacelle

The viscous drag coefficient C_{DV} of the nacelle is calculated as explained earlier for cruise conditions. For $M_\infty = 0.8$ and different angles of attack, the results are given in Fig. 12. For the asymmetric flow cases ($\alpha \geq 0$ deg), the values of C_{DV} are averaged from the various radial section values due to different transition locations. As the transition location in the region of the section ($\theta = 0$ deg) is moving upstream with increasing angle of attack, the drag coefficient is increased, as shown in Fig. 12.

The development of the drag coefficient with Mach number M_∞ at $\alpha = 0$ deg is shown in Fig. 13 as the sum of viscous drag and wave drag. At Mach numbers greater than 0.8, the pressure distributions show considerable shock waves, which generate additional wave drag. As explained earlier, the wave drag coefficient C_{DW} is estimated and plotted in Fig. 13 for $M_\infty > 0.8$.

To show the effect of the laminar boundary layer, drag values have been computed with both the assumptions of natural transition and fixed transition at $x/c = 0.05$. With natural transition, the nacelle drag decreases with increasing Mach number. This is due to the larger favorable pressure gradients at higher Mach numbers and, consequently, a transition location further downstream. For $M_\infty > 0.8$, there is a sudden drag rise due to the strong shocks. In the case of fixed transition, the viscous drag remains almost constant for Mach numbers up to $M_\infty = 0.8$.

If the drag coefficients for natural laminar flow and fixed transition are compared, a drag reduction of $\Delta C_D = 0.012$ at $M_\infty = 0.8$ is obtained. With reference to the overall drag of an Airbus A320 (two nacelles, wing area of 122.4 m^2), the drag reduction is $\Delta C_{D,A/C} = 0.0011$. For an estimated total aircraft drag value of $C_{D,A/C} = 0.032$, the drag reduction by laminar flow nacelles is about 3.5%.

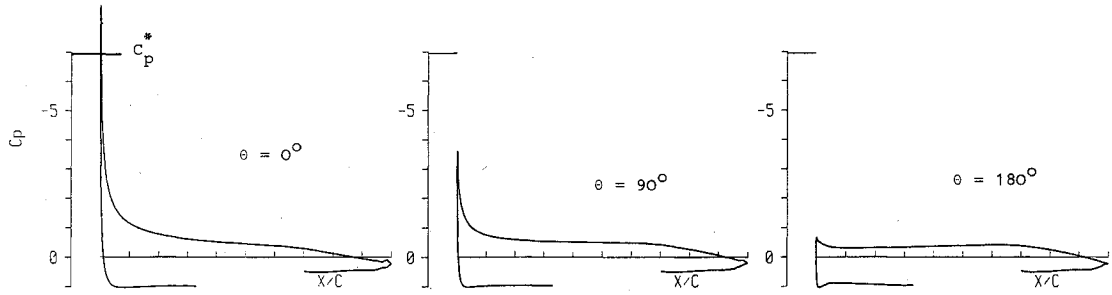

Fig. 11 Pressure distributions on three sections of nacelle LN1 (M_∞ = 0.3, α = 9 deg, and ϵ = 0.2).

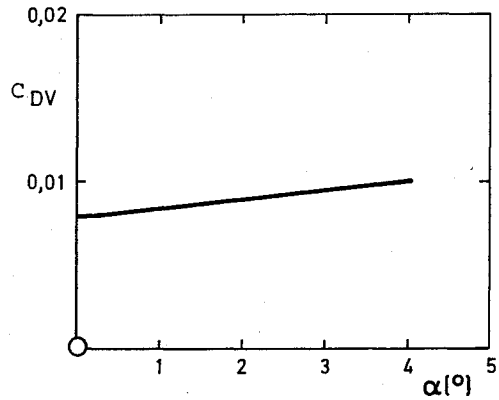

Fig. 12 Influence of angle of attack on viscous drag, C_{DV}, of nacelle LN1, natural transition (M_∞ = 0.8, Re = 20 × 10^6, and ϵ = 0.76).

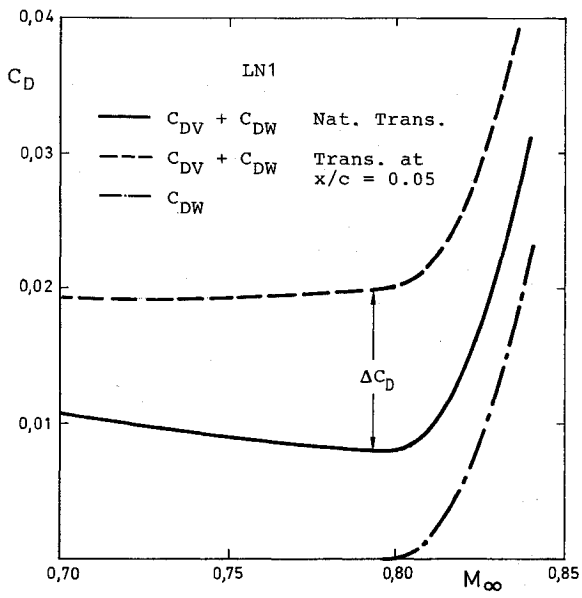

Fig. 13 Influence of Mach number on viscous drag, C_{DV}, and wave drag, C_{DW}, for outer contour nacelle LN1 (α = 0 deg, Re = 20 × 10^6, and ϵ = 0.76).

Conclusions and Recommendations

The present feasibility study has shown that

1) Natural laminar flow nacelles for cruise conditions of M_∞ = 0.8 and Re = 20 × 10^6 can be designed, taking into account takeoff and landing design requirements.

2) Laminar boundary layers of up to 60% of nacelle chord can be achieved.

3) Estimated drag reduction for the cruise conditions of an A320 aircraft is about 3.5% of total aircraft drag.

It is anticipated that further improvement in the design can be obtained if the restriction to an axisymmetric nacelle is dropped. This is because the flow conditions at the design points are different on the upper and lower sides of the nacelle.

Since the present study is based exclusively on numerical flow methods, it remains to be shown that the present design works in real flow. The next step is then to realize a laminar flow nacelle mounted on a real transport aircraft. For this, several additional problems must be considered.

1) Interference: The design of a laminar flow nacelle mounted under the wing of a transport must take into account wing-pylon interference effects.

2) Engine noise and vibration: It should be noted that, for the present design, a certain safety margin in transition prediction is incorporated, which should account for the additional disturbances created by noise and vibration.

3) Contamination: The problem of contamination of the nacelle leading edge by dust and insects must be considered. Development of systems for wing leading edges is underway.

4) Maintenance: The front of the outer nacelle surface must be free from steps and cover plates or maintenance holes. The holes should be arranged as far downstream as possible.

Acknowledgment

The authors would like to thank Airbus Industries for the permission to publish the present results, which were obtained under contract P. 304019.

References

[1]Redeker, G., Horstmann, K. H., Köster, H., and Quast, A., "Investigations on High Reynolds Number Laminar Flow Airfoils," *Proceedings of 15th ICAS Congress,* AIAA, New York, 1986, pp. 73-85.

[2]Rossow, C.-C., Kroll, N., Radespiel, R., and Scherr, S., "Investigation of the Accuracy of Finite-Volume Methods for 2- and 3-Dimensional Flows," AGARD-CP-437, Vol. 2, 1988, p. 14.

[3]Rossow, C.-C., "Berechnung von Strömungsfeldern durch Lösung der Euler-Gleichungen mit einer neuen Finite-Volumen Diskretisierungsmethode," DLR, Cologne, FRG, Rept. DLR-FB 89-38, 1989.

[4]Radespiel, R., "Calculation of the Flow Around Powered High Bypass Ratio Nacelles Using an Euler Code," DLR, Cologne, FRG, Rept. DLR-IB 129-87/25, 1987.

[5]Rotta, J.-C., "FORTRAN IV—Rechenprogramm für Grenzschichten bei kompressiblen und achsensymmetrischen Strömungen," Rept. DLR-FB 71-51, 1971.

[6]Skrokowski, A. J., and Orzag, S. A., "Mass Flow Requirements for LFC Wing Design," AIAA Paper 77-1222, 1977.

[7]Redeker, G., and Horstmann, K. H., "Die Stabilitätsanalyse als Hilfsmittel beim Entwurf von Laminarprofilen," DGLR, Bonn, FRG, Rept. DGLR-Bericht 86-03, 1986, pp. 317-348.

[8]Wichmann, G., "Einfluss der Rotationssymmetrie auf die Grenzschiechtentwicklung der Aussenströmung bei gondelähnlichen Konfigurationen," DLR, Cologne, FRG, Rept. DLR-IB 129-87/10, 1987.

[9]Squire, H. B., and Young, A. D., "The Calculation of the Profile Drag of Aerofoils," Royal Aircraft Establishment, Bedford, England, Rept. 1838, 1937.

[10]Eppler, R., and Somers, D. M., "A Computer Program for the Design and Analysis of Low-Speed Airfoils," NASA TM-80210, 1980.